journal

J. Am. Ceram. Soc., **85** [8] 2019–24 (2002)

Rate Effects in Critical Loads for Radial Cracking in Ceramic Coatings

Chul-Seung Lee and Do Kyung Kim*

Department of Materials Science and Engineering, Korea Advanced Institute of Science and Technology, Yusong, Taejon 305-701, Korea

Jose Sánchez and Pedro Miranda

Departamento Electrónica e Ingeniería Electromecánica, Escuela de Ingenierías Industriales, Universidad de Extremadura, 06071 Badajoz, Spain

Antonia Pajares

Departamento de Física, Facultad de Ciencias, Universidad de Extremadura, 06071 Badajoz, Spain

Brian R. Lawn*

Materials Science and Engineering Laboratory, National Institute of Standards and Technology, Gaithersburg, Maryland 20899

Rate effects in the Hertzian contact loading of model glass/polycarbonate and silicon/polycarbonate bilayers bonded by epoxy adhesive are examined. Glass is used because of its high susceptibility to slow crack growth, making this conventional contribution to the rate dependencies easy to distinguish. Silicon is used as a control material with effectively no slow crack growth. Abrasion damage is introduced into the undersurfaces of the brittle coating layers to provide controlled flaws for the initiation of radial cracks from flexural stresses introduced by the contact loading. Critical loads are measured as a function of loading rate. Comparative flexural strength tests on free-standing abraded specimens show a pronounced rate dependence in the glass but none in the silicon, entirely consistent with slow crack growth effects. The glass/polycarbonate bilayer critical load data show a similar trend, but with stronger loading-rate dependence, suggesting an extraneous contribution to the kinetics from the adhesive/substrate. The silicon/polycarbonate bilayer data also show a loading-rate dependence, albeit much smaller, confirming this last conclusion. Data from cyclic contact tests on the glass/polycarbonate bilayers coincide with the loading-rate data on lifetime plots, eliminating the likelihood of a mechanical component in the fatigue response. It is concluded that the adhesive/substrate contribution is viscoelastic in nature, from energy-dissipating (but noncumulative) anelastic deformation during the cyclic loading. Critical load tests on bilayers with different exposures to external water show no influence of external environment, suggesting that internal moisture is responsible for the slow crack growth in the glass-coating bilayers.

I. Introduction

RECENT evaluations have been made of critical loads to produce Hertzian contact damage in bilayers of ceramic coatings bonded to soft polymer and metal substrates.[1–7] Such damage is relevant to the failure of dental crowns, hip prostheses, laminated glasses, thermal barrier coatings, hard disks, and other engineering layer structures. The usual near-contact top-surface damage modes documented in studies on monolithic materials,[8,9] i.e., cone cracks (in fine-grain ceramics and glasses) and quasi plasticity (in coarse, tough ceramics), persist in ceramic coating structures. But potentially more damaging are radial cracks initiating at the lower ceramic surface (i.e., the coating/substrate interface), especially in thinner coatings. Radial cracking is believed to be the primary cause of failure in dental crowns,[10–12] for instance. The tensile stress state at the coating undersurface in concentrated loading is analogous to that in a biaxial strength test, attributable to flexure of the coating on its compliant support. One difference is that in the bilayer system these tensile stresses are somewhat localized below the indenter, so that propagating cracks tend to be stable[5]—initiation does not usually take the bilayer to spontaneous failure. Bilayer studies have proved useful in determining key variables such as layer thickness, material properties, surface flaw state, etc., and have led to the development of explicit fracture mechanics relations for the critical loads in terms of these variables.

Until now, attention in bilayer contact testing has focused on single-cycle loading at some fixed load rate or crosshead speed. Practical layer structures may be subject to premature failure in sustained or repeat loading during service, resulting in finite lifetimes. How much of this failure may be ascribed to slow growth of the radial cracks that initiate from flaws in the undersurfaces of ceramic coatings remains to be addressed. Rate effects of this kind are strongly evident in strength characteristics in conventional flexural strength tests. Since slow crack growth is generally associated with the chemical influence of water,[13–15] accessibility of moisture to the coating/substrate interface where the radial cracks originate becomes an issue. Slow crack growth has certainly been confirmed as a primary rate-dependent mechanism in the growth of cone cracks at the top surface of monolithic ceramics,[16,17] where moisture has no difficulty entering the crack mouth. The influence of moisture is also manifest to some extent in quasi-plastic zones, but there micromechanical degradation of the microstructure is a more dominant mode of damage accumulation.[18] Questions then arise as to whether competing mechanical

D. B. Marshall—contributing editor

Manuscript No. 187349. Received November 6, 2001; approved April 30, 2002.

This study was supported in part by NIST internal funds, by the Korea Ministry of Education (Brain Korea 21 Program of KAIST), by the Junta de Extremadura-Consejeria de Educación, Ciencia y Tecnología y el Fondo Social Europeo, Spain (Grant IPR00A084), and by the U.S. National Institute of Dental Research (Grant PO1DE10976).

*Member, American Ceramic Society.

influences can arise in bilayer systems, from some form of irreversible rate- or cycle-dependent damage in the sublayers, progressively reducing the effective modulus of the support base and thereby allowing buildup of tension in the coating undersurface—e.g., from cumulative plasticity[19] or viscoelastic relaxation.[20] Accordingly, in ceramic/substrate bilayer systems care needs to be taken to distinguish between chemical effects from slow crack growth in the coating and mechanical effects from dissipative processes in the support substrate.

In this paper we describe the results of Hertzian contact tests on ceramic/substrate bilayers aimed specifically at determining rate effects. For our model system we use glass/polycarbonate bilayers, bonded by a thin layer of epoxy adhesive, from an earlier study.[2] Abrasion flaws are introduced into the glass undersurfaces before bonding, to provide controlled flaws and thus to reduce scatter in the critical loads to produce radial cracks. Advantages of this system, apart from the fact that its mechanics are well studied, are twofold: first, both the polycarbonate and the adhesive are transparent, making *in situ* observation of the radial cracks straightforward; second, the fracture of glass is particularly susceptible to moisture,[13,14] so that slow crack growth effects may be easily distinguished. Tests are conducted by loading a blunt indenter on the bilayer top surface in single-cycle loading at constant stressing rates, and in multicycle loading at prescribed frequencies. Critical loads to induce radial fractures are then measured as a function of contact duration. Comparative tests on silicon/polycarbonate bilayers are conducted as a control, making use of the relative immunity of silicon to moisture-assisted slow crack growth[21] to isolate any mechanical from chemical contributions to the fatigue. Subsidiary constant stressing rate tests on glass/polycarbonate bilayers with different exposures to water are used to ascertain the influence of external environmental conditions. We will argue that most of the fatigue in the glass-coating bilayers is indeed due to chemically assisted slow crack growth, associated with residual internal water at the ceramic/adhesive–substrate interface. However, an extraneous contribution associated with viscoelasticity effects in the adhesive–substrate underlayer could become an important factor in bilayer ceramic coating systems with smaller slow crack growth susceptibility.

II. Rate Effect Due to Slow Crack Growth—Fracture Mechanics

Begin by considering rate effects from slow crack growth alone. Consider a ceramic coating of thickness d and Young's modulus E_c bonded with thin adhesive onto a thick compliant substrate of modulus E_s, subjected to a concentrated load P at the top surface (Fig. 1). The load causes the coating to flex on the compliant support, inducing a tensile stress at the lower coating surface at the contact axis[2]

$$\sigma = (P/Bd^2)\log(CE_c/E_s) \tag{1}$$

where B and C are dimensionless coefficients.[4]

Suppose the lower surface of the ceramic below the indenter contains flaws of characteristic dimension c_f that can serve as initiation sites for radial cracks. In earlier analyses it has been assumed that the critical load to initiate radial cracking at the lower ceramic surface from such a flaw occurs when σ in Eq. (1) equals the bulk strength of the ceramic.[3,4,22] Thus, in effect, the critical load to produce a radial crack is a direct measure of the coating strength. This assumption has been validated by comparing critical subsurface stresses with actual strength data obtained from analogous tests on the same coating materials in four-point bending (except for very large, or sparse flaws—not applicable here).[5] It is contingent on the existence of a sufficient density of flaws in the tensile region (a condition that can be violated in thinner coatings, i.e., $\ll$1 mm for abraded glass, but is not an issue here).[7]

It is presumed in previous critical load analyses that the strength of ceramics is a well-defined, equilibrium quantity, whereas in reality it is usually load-rate dependent. Here we outline an analysis based on the hypothesis that any rate effects are due exclusively to slow crack growth of prepresent flaws, governed by a crack velocity equation.[13,15,23] As indicated (Section I), slow crack growth is generally attributable to intrusion of water molecules into the crack walls. Such intrusion implies access of water molecules to the flaw mouth, from either internal or external moisture. The question arises as to whether such access exists at the lower ceramic surface in the bilayer structure—the substrate and associated bonding adhesive might have been expected to provide some "protection" from the external environment. We can test this notion in the present study by conducting prescribed load-rate tests on model bilayer coating/substrate systems and looking for any deviations from predicted behavior. Such deviations have been used to identify the presence of extraneous sources of fatigue in cyclic contact tests on monolithic, tough, coarse-grain ceramics—in that case, from cumulative quasi plasticity.[16]

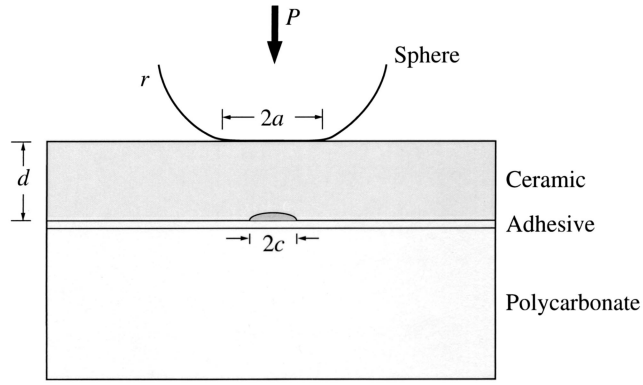

Fig. 1. Schematic of bilayer test configuration, showing ceramic coating layer of thickness d bonded with thin epoxy adhesive interlayer to polycarbonate substrate. Bilayer is loaded with indenter of radius r at top surface, contact radius a. Radial crack initiates from surface flaw, characteristic dimension c, at lower ceramic surface.

Accordingly, suppose that a flaw of initial size c_f in the lower ceramic surface in Fig. 1 is subject to time-dependent extension $c(t)$ from an applied stress $\sigma(t)$ according to a velocity relation[23]

$$v = v_0(K/T)^N \tag{2}$$

with K the stress-intensity factor, T the toughness (here assumed single-valued, $T = K_{IC}$), and N and v_0 crack velocity exponent and coefficient. Assuming the flaw to be free of any extraneous residual stress, the stress-intensity factor on the flaw in the range $c_f \leq c \ll d$ is

$$K = \psi\sigma c^{1/2} \tag{3}$$

with ψ a crack geometry coefficient. Combining Eqs. (1) to (3) and integrating over crack length between $c = c_f$ and $c = c_*$ (corresponding to final instability at $K = T$) we obtain, in the approximation $N \gg 1$ (so that terms in c_* are negligibly small)

$$\int_0^{t_R} [P(t)]^N \, dt = A \tag{4}$$

with $A = \{1/[(N/2-1)v_0 c_f^{(N/2-1)}]\}[BTd^2/\psi\log(CE_c/E_s)]^N$ a load- and time-independent quantity.

It remains only to specify $P(t)$. Here we are interested in two contact test configurations:

(i) *Constant loading rate ("dynamic fatigue")*: The specimen is loaded at a constant rate $\dot{P}$ until initiation of a radial crack at critical load P_m

$$P(t) = \dot{P}t = (P_m/t_R)t \tag{5}$$

where t_R is the elapsed time to produce the radial crack. Substituting into Eq. (4) and integrating yields

$$P_m^N t_R = A(N+1) \tag{6}$$

or, alternatively,

$$P_m = [A(N+1)\dot{P}]^{1/(N+1)} \tag{7}$$

(ii) *Constant frequency ("cyclic fatigue")*: The specimen is loaded sinusoidally between $0 \le P \le P_m$ at a constant frequency f, i.e.,

$$P(t) = (P_m/2)[1 - \sin(2\pi ft - \pi/2)] \tag{8}$$

until initiation of a radial crack at time t_R. Substituting into Eq. (4) and integrating, we obtain[16]

$$P_m^N t_R = 2AN^{0.47} \tag{9}$$

by analogy with Eq. (6).

Noting Eq. (1), the dynamic fatigue relation Eq. (7) can be reduced to a more familiar form for plates subjected to a critical flexural tensile stress

$$\sigma_m = [A_0(N+1)\dot{\sigma}]^{1/(N+1)} \tag{10}$$

where $A_0 = (T/\psi)^N/[(N/2-1)\nu_0 c_f^{(N/2-1)}]$.

We reiterate that these equations are based on the assumption that the fracture kinetics are determined exclusively by slow crack growth, free of residual stresses acting on the flaws. Any extraneous kinetic contribution from the adhesive/substrate will increase the rate dependency, so that experimentally measured exponents N' evaluated from Eqs. (6), (7), and (9) may be lower than the true crack velocity exponent N. Moreover, if the flaws are generated by elastic–plastic microcontacts,[15,21,24–28] the value of N' may be depressed still further, dependent on the intensity of the residual contact stress—for surface abrasion flaws, this contribution is typically small, because of stress relaxation from chipping around the flaw sites.[29]

III. Experiments

Brittle coating layers were prepared from soda–lime glass microscope slides (Fischer Scientific, Pittsburgh, PA) of dimensions 75 mm × 25 mm × 1 mm, and from polished (001) monocrystalline silicon plates (Virginia Semiconductors, Fredericksburg, VA) of the same thickness and cut to the same lateral dimensions. The lower surfaces of the bulk of the coating layers were lightly abraded with grade 600 SiC grit to introduce controlled flaws for ensuing radial cracking.[7,30] An epoxy resin (Harcos Chemicals, Bellesville, NJ) was then used to bond the layers to a clear polycarbonate base 12.5 mm thick (Hyzod, AIN Plastics, Norfolk, VA). The specimens were lightly clamped during curing to keep the adhesive layer thin, ≈10 μm. Most specimens were bonded in air, but some were bonded *in situ* in a dry box (<25% humidity) after allowing all components 2 days to equilibrate within the enclosure.

Contact tests on the glass/polycarbonate and silicon/polycarbonate bilayers were made using a tungsten carbide (WC) indenting sphere of radius $r = 3.18$ mm mounted into the crosshead of a mechanical loading machine. (Some tests were made with a flat of diameter 0.9 mm ground on the sphere, to enable better visualization of contact area.) The bilayers were mounted onto glass slabs 6 mm thick to provide additional base support during indentation. Several indentation tests could be made on any one bilayer surface. Load data were recorded digitally at a rate of 500 s^{-1}, with a resolution of better than 0.1 N. Constant loading rate tests over a range $\dot{P} = 0.01$ to 1000 $N{\cdot}s^{-1}$ were conducted on a screw-driven Instron testing machine (Model 5500R, Instron Corp, Canton, MA). Load rates were determined from the near-linear regions of the recorded load–time responses $P(t)$. The incidence of radial cracking in the lower coating surface was viewed from below, through a 3 mm diameter hole in the specimen support stage, using a microscope zoom system (Optem, Santa Clara, CA) with its optical axis carefully aligned along the load axis and mounted into a video camcorder (Canon XL1, Canon, Lake Success, NY). These observations enabled direct measurement of critical loads P_m. Distinctive load drops in the $P(t)$ responses, typically 5 N in magnitude, allowed more accurate determinations of P_m at the faster load rates. Corresponding fracture times $t_R = P_m/\dot{P}$ were calculated from the measured critical loads at the different load rates.

Some cyclic tests were made on glass/polycarbonate bilayers on a servo-hydraulic machine (Model 8502, Instron Corp, Canton, MA) at frequencies $f = 0.1$, 1, and 10 Hz. At each frequency, four maximum loads, $P_m = 75$, 90, 110, and 120 N, were used. Again, the specimens were observed from below, and the time t_R to radial cracking was duly measured for each test condition.

The bulk of the tests were run in laboratory atmosphere. Additional dynamic fatigue tests were run on glass/polycarbonate bilayers in water, to investigate the role of external environment. These tests included specimens presoaked in water for prescribed periods, followed by immediate testing either in air (after quick surface drying) or in the same water bath.

In addition, some comparative four-point bend tests were conducted on free-standing glass bars 35 mm × 12 mm × 1 mm cut from the same slides and silicon bars 60 mm × 8 mm × 1 mm cut from the same plates as above. Specimen edges were chamfered using 6 μm diamond paste. The center regions of the prospective lower tensile surfaces were preabraded in the same way as the bilayer specimens. Constant loading rate tests to failure were then conducted in four-point flexure, inner and outer spans 10 and 20 mm (glass) and 20 and 40 mm (silicon), and strengths σ_m calculated from the breaking loads.

IV. Results and Analysis

(1) Four-Point Flexure Tests

To establish a base line for analyzing the bilayer test data, we first present dynamic fatigue results from four-point flexure tests on the free-standing abraded soda–lime glass and silicon bars. Data are plotted in Fig. 2 (means and standard deviations, minimum of five specimens). Linear fits to the raw data in logarithmic coordinates, in accordance with Eq. (10), are shown as the solid lines. These fits yield mean and standard error evaluations $N = 18.1 \pm 1.1$ (slope 0.0524 ± 0.0032) for glass and $N \approx \infty$ effectively (slope

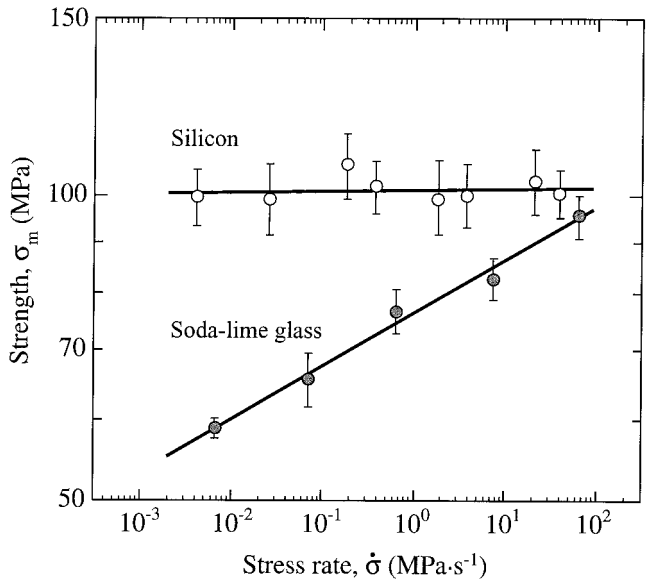

Fig. 2. Plot of strength σ_m versus stressing rate $\dot{\sigma}$ for preabraded soda–lime glass bars (filled symbols) and silicon bars (unfilled symbols). Error bars are means and standard deviations, minimum of five specimens. Solid lines are linear logarithmic best fits to Eq. (10).

0.0012 ± 0.0034) for silicon. The N value for soda–lime glass is close to the "true" crack velocity exponent $N = 18.0 \pm 0.5$ from independent evaluations,[14,26,31] suggesting insignificant residual contact stresses around the abrasion flaws. For the silicon, the infinite value of N is consistent with the absence of any significant intrinsic slow crack growth in this material.

(2) Bilayer Tests

Subsurface views of radial crack patterns in glass and silicon bilayers, obtained using spherical indenters with machined flats, are shown in Fig. 3. In glass (Fig. 3(a)), the circular contact area is clearly visible through the transparent coating. The radial crack patterns are the same as observed previously in isotropic glasses and ceramics,[2,4,30] i.e., centered close to the load axis and geometrically orientation-independent indent to indent. In silicon (Fig. 3(b)), the contact area is not detectable through the opaque coating. However, the radial cracks always initiated close to the center of the optical field of view, i.e., close to the contact axis. In this material the radial cracks always showed orthogonal traces on the (001) surfaces, and always with the same orientation from indent to indent, consistent with {111} cleavage.[32]

Plots of data for radial crack critical load P_m as a function of loading rate $\dot{P}$ from dynamic fatigue tests in air are shown for the glass/polycarbonate and silicon/polycarbonate bilayers in Fig. 4 (means and standard deviations, minimum of five tests). Solid lines are linear best fits to the raw data, in logarithmic coordinates. In accordance with Eq. (7), these best fits yield $N' = 16.0 \pm 0.7$ for glass and $N' = 66 \pm 11$ for silicon (means and standard errors). These N' values are lower than the corresponding N values obtained from the flexure data in Fig. 2 (Section IV(1)). Computation of 95% confidence limits for the data fits confirms that these differences are significant—i.e., there is a real contribution to the rate effect from the adhesive/substrate in the bilayer data.

Figure 5 compares results of the constant loading rate tests on glass/polycarbonate bilayers from Fig. 4 (using $t_R = P_m/\dot{P}$) with those of cyclic loading tests (three frequencies) on the same bilayers, for tests in air (filled symbols). The solid line is a prediction from Eq. (9) using the parametric evaluation from the best-fit line to the glass/polycarbonate data in Fig. 4. The cyclic data represent means for a minimum of 15 tests per condition (standard deviations omitted). No significant departures from the solid line are observed for the cyclic data, implying the absence of any mechanical fatigue effect under the specified test conditions. Also included in Fig. 5 are data from constant loading rate tests conducted on dry-box-prepared bilayers (unfilled symbols). In this instance, the dashed curve is a best fit but with the same N' value as the air-prepared specimens.

Results of tests on glass/polycarbonate bilayers tested in different water environments are shown in the bar diagram of Fig. 6, at two loading rates. The results are for tests in air (A), in air with water presoak (AP), in water (W), and in water with presoak (WP), presoak times indicated (days). Data are means and standard deviations, minimum of eight tests per condition. Whereas results for the two loading rates are substantially different within the experimental scatter, no such difference is apparent within each loading rate data set. These results suggest no external environmental influence on the radial fracture kinetics.

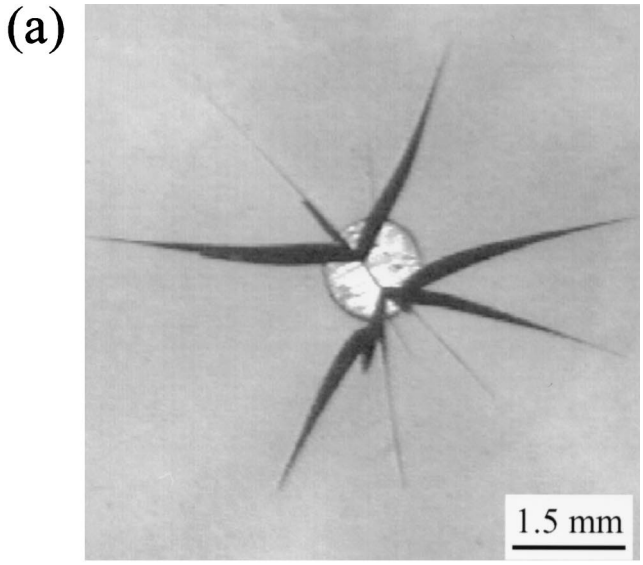

Fig. 3. *In situ* photographs of radial cracks in brittle coatings, $d = 1$ mm, viewed from below through clear polycarbonate substrates, thickness 12.7 mm. Indentation made with WC sphere of radius $r = 3.18$ mm containing ground flat of 0.9 mm diameter. (a) Soda–lime glass, load $P = 125$ N, random orientation relative to load axis indent to indent. Note contact circle through transparent coating. (b) Silicon, $P = 136$ N, cracks orthogonally aligned along traces of {111} cleavage planes on (001) surfaces.

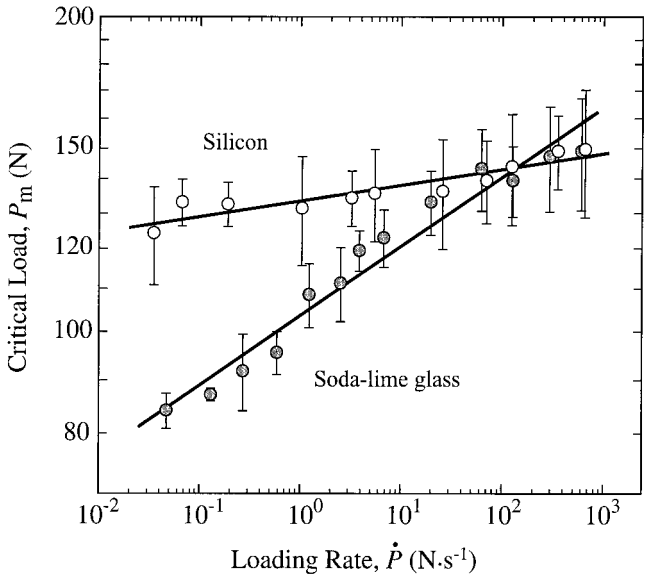

Fig. 4. Plot of critical load P_m for radial cracking as function of loading rate $\dot{P}$ for coatings of soda–lime glass (filled symbols) and silicon (unfilled symbols) bonded to polycarbonate substrates. Indentations with WC sphere, radius $r = 3.18$ mm, tests in air. Data points are means and standard deviations of a minimum of five tests per loading rate for each condition. Solid lines are linear best fits in logarithmic coordinates.

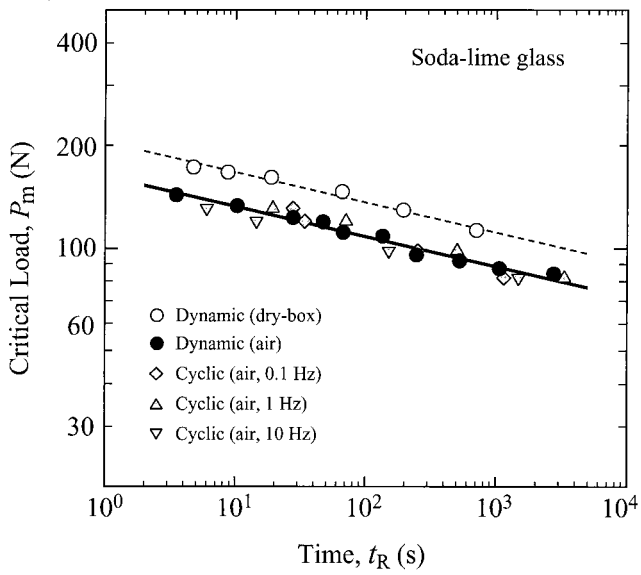

Fig. 5. Plot of maximum contact load P_m as function of time t_R to radial cracking for soda–lime glass coatings bonded to polycarbonate substrates. Indentations with WC sphere, radius $r = 3.18$ mm, all tests in air. Filled symbols are data for air-prepared bilayers, cyclic loading tests (minimum of 15 tests per maximum load) at three frequencies (indicated) and constant loading rate tests (from Fig. 4)—solid line generated from parameter fit to glass data in Fig. 4 using Eq. (9). Unfilled symbols are data for dry-box-prepared specimens, constant loading rate tests—dashed line is simply parallel-shifted solid line through these data. (Standard deviation error bars not included, to avoid data overlap.)

V. Discussion

We have demonstrated the existence of rate effects in the critical contact loads to initiate radial cracks at the undersurfaces of soda–lime glass and silicon coatings bonded to compliant polycarbonate substrates (Fig. 4). Constant loading rate experiments show rate effects in crack initiation from controlled abrasion flaws, amounting to a drop of a factor of 2 or so over some 4 decades in loading rate in the glass bilayer data. A much smaller, but not insignificant, effect is observed in the silicon bilayer data.

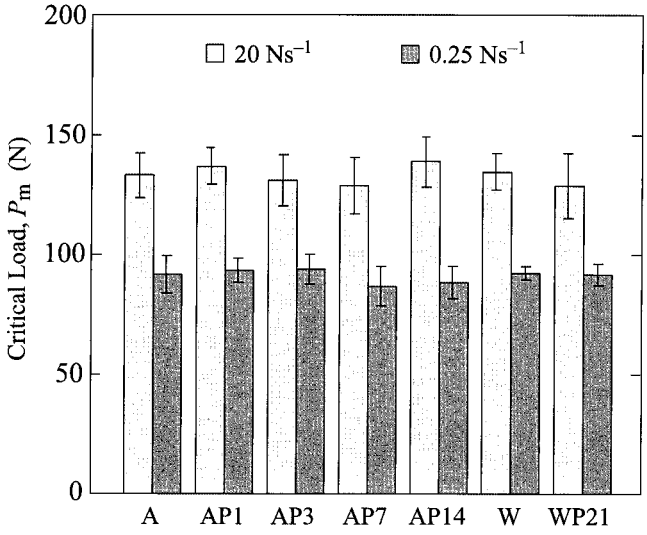

Fig. 6. Bar chart comparing critical loads P_m to radial cracking in soda–lime glass coatings bonded to polycarbonate substrates, under different environmental test conditions: air (A), air with water presoak (AP), water (W), and water with presoak (WP)—presoak times indicated (days). Indentations with WC sphere, radius $r = 3.18$ mm.

Comparative flexural strength tests on free-standing glass bars (Fig. 2) indicate similar trends in the glass data, consistent with slow crack growth in the abrasion flaws before crack initiation. Similar flexural strength tests on silicon, on the other hand, show no measurable rate effect. The comparative data on silicon suggests that while slow crack growth is a major contributor to the fatigue in glass, there must be some secondary contribution from the adhesive/substrate support in the bilayer structures.

Further comparison of the glass/polycarbonate bilayer data at constant loading rate with those for cyclic loading (Fig. 5) shows no discernible differences for specimens prepared in air. This suggests that any rate effect associated with the adhesive/polycarbonate substrate is not cumulative. A simple finite element analysis using a previously described algorithm for the indentation of glass-coating bilayer structures[22] indicates sublayer stresses well below the yield points of the polycarbonate and adhesive materials, confirming the absence of plasticity and thus eliminating the likelihood of "cyclic creep."[19] This does not preclude viscoelasticity, which can lead to closed-loop load/unload hysteresis (anelasticity) without residual, cumulative deformation. Such a process could allow greater coating deflections and thus enhanced tensile stresses at the undersurface of the flexing coating layer at slower loading rates, potentially accounting for the sublayer rate effects alluded to in the preceding paragraph. This is an area of research that warrants closer attention, especially in systems with high polymeric components in the substrates, and for coatings with relatively small slow crack growth (high N) where the viscoelastic contribution could become a larger part of the rate effect.

The extraneous test environment does not seem to influence the critical loads for radial cracking in the glass/polycarbonate bilayers (Fig. 6), implying that external water does not diffuse at any significant rate along the adjoining interfaces or through the polycarbonate. Yet tests at different loading rates still demonstrate significant shifts in the data. This implies short-range migration of internal water to the critical interface region. Such short-range transport of water has been proposed for polymer-coated optical fibers,[33] by diffusion of extraneous moisture through the coating, and dental crown systems, from sources in the live dentin through the adjoining dental cement interlayer.[10] This conclusion is consistent with the shift in constant loading rate data to higher P_m values for dry-box-prepared specimens in Fig. 5, attributable to a reduced concentration of moisture in the adhesive/substrate support.

Finally, we acknowledge our restriction in the fracture mechanics analysis of Section II to ceramic materials with single-valued toughness, i.e., no R-curve.[15] This should not be a major limitation in practical applications in which ceramic coating materials are chosen for high wear resistance (bearings) or aesthetics (porcelain-veneered crowns), where hardness and strength supersede toughness as primary material properties.

Acknowledgments

We acknowledge useful discussions with Hong Zhao and Fernando Guiberteau.

References

[1]L. An, H. M. Chan, N. P. Padture, and B. R. Lawn, "Damage-Resistant Alumina-Based Layer Composites," *J. Mater. Res.*, **11** [1] 204–10 (1996).

[2]H. Chai, B. R. Lawn, and S. Wuttiphan, "Fracture Modes in Brittle Coatings with Large Interlayer Modulus Mismatch," *J. Mater. Res.*, **14** [9] 3805–17 (1999).

[3]B. R. Lawn, K. S. Lee, H. Chai, A. Pajares, D. K. Kim, S. Wuttiphan, I. M. Peterson, and X. Hu, "Damage-Resistant Brittle Coatings," *Adv. Eng. Mater.*, **2** [11] 745–48 (2000).

[4]Y.-W. Rhee, H.-W. Kim, Y. Deng, and B. R. Lawn, "Contact-Induced Damage in Ceramic Coatings on Compliant Substrates: Fracture Mechanics and Design," *J. Am. Ceram. Soc.*, **18** [5] 1066–72 (2001).

[5]H.-W. Kim, Y. Deng, P. Miranda, A. Pajares, D. K. Kim, H.-E. Kim, and B. R. Lawn, "Effect of Flaw State on the Strength of Brittle Coatings on Soft Substrates," *J. Am. Ceram. Soc.*, **84** [10] 2377–84 (2001).

[6]H. Zhao, X. Hu, M. B. Bush, and B. R. Lawn, "Cracking of Porcelain Coatings Bonded to Metal Substrates of Different Modulus and Hardness," *J. Mater. Res.*, **16** [5] 1471–78 (2001).

[7]P. Miranda, A. Pajares, F. Guiberteau, F. L. Cumbrera, and B. R. Lawn, "Role of Flaw Statistics in Contact Fracture of Brittle Coatings," *Acta Mater.*, **49** [18] 3719–26 (2001).

[8]B. R. Lawn, N. P. Padture, H. Cai, and F. Guiberteau, "Making Ceramics 'Ductile'," *Science*, **263**, 1114–16 (1994).
[9]Y.-W. Rhee, H.-W. Kim, Y. Deng, and B. R. Lawn, "Brittle Fracture versus Quasi-Plasticity in Ceramics: A Simple Predictive Index," *J. Am. Ceram. Soc.*, **84** [3] 561–65 (2001).
[10]J. R. Kelly, "Clinically Relevant Approach to Failure Testing of All-Ceramic Restorations," *J. Prosthet. Dent.*, **81** [6] 652–61 (1999).
[11]Y. G. Jung, S. Wuttiphan, I. M. Peterson, and B. R. Lawn, "Damage Modes in Dental Layer Structures," *J. Dent. Res.*, **78** [4] 887–97 (1999).
[12]B. R. Lawn, Y. Deng, and V. P. Thompson, "Use of Contact Testing in the Characterization and Design of All-Ceramic Crown-like Layer Structures: A Review," *J. Prosthet. Dent.*, **86** [5] 495–510 (2001).
[13]S. M. Wiederhorn, "Influence of Water Vapor on Crack Propagation in Soda–Lime Glass," *J. Am. Ceram. Soc.*, **50** [8] 407–14 (1967).
[14]S. M. Wiederhorn and L. H. Bolz, "Stress Corrosion and Static Fatigue of Glass," *J. Am. Ceram. Soc.*, **53** [10] 543–48 (1970).
[15]B. R. Lawn, *Fracture of Brittle Solids*. Cambridge University Press, Cambridge, U.K., 1993.
[16]D. K. Kim, Y.-G. Jung, I. M. Peterson, and B. R. Lawn, "Cyclic Fatigue of Intrinsically Brittle Ceramics in Contact with Spheres," *Acta Mater.*, **47** [18] 4711–25 (1999).
[17]J.-G. Yeo, K. S. Lee, and B. R. Lawn, "Role of Microstructure in Dynamic Fatigue of Glass-Ceramics After Contact with Spheres," *J. Am. Ceram. Soc.*, **83** [6] 1545–47 (2000).
[18]K. S. Lee, Y.-G. Jung, I. M. Peterson, B. R. Lawn, D. K. Kim, and S. K. Lee, "Model for Cyclic Fatigue of Quasi-Plastic Ceramics in Contact with Spheres," *J. Am. Ceram. Soc.*, **83** [9] 2255–62 (2000).
[19]S. Suresh, *Fatigue of Materials*. Cambridge University Press, Cambridge, U.K., 1991.
[20]S. J. Bennison, A. Jagota, and C. A. Smith, "Fracture of Glass/Poly(vinyl butyral) (Butacite®) Laminates in Biaxial Flexure," *J. Am. Ceram. Soc.*, **82** [7] 1761–70 (1999).
[21]B. R. Lawn, D. B. Marshall, and P. Chantikul, "Mechanics of Strength Degrading Flaws in Silicon," *J. Mater. Sci.*, **16** [7] 1769–75 (1981).
[22]P. Miranda, A. Pajares, F. Guiberteau, F. L. Cumbrera, and B. R. Lawn, "Contact Fracture of Brittle Bilayer Coatings on Soft Substrates," *J. Mater. Res.*, **16** [1] 115–26 (2001).
[23]S. M. Wiederhorn, "Subcritical Crack Growth in Ceramics"; pp. 613 in *Fracture Mechanics of Ceramics*, Vol. 2. Edited by R. C. Bradt, F. F. Lange, and D. P. H. Hasselman. Plenum, New York, 1974.
[24]D. B. Marshall and B. R. Lawn, "Residual Stress Effects in Sharp-Contact Cracking: I, Indentation Fracture Mechanics," *J. Mater. Sci.*, **14** [8] 2001–12 (1979).
[25]D. B. Marshall, B. R. Lawn, and P. Chantikul, "Residual Stress Effects in Sharp-Contact Cracking: II, Strength Degradation," *J. Mater. Sci.*, **14** [9] 2225–35 (1979).
[26]D. B. Marshall and B. R. Lawn, "Flaw Characteristics in Dynamic Fatigue: The Influence of Residual Contact Stresses," *J. Am. Ceram. Soc.*, **63** [9–10] 532–36 (1980).
[27]B. R. Lawn, A. G. Evans, and D. B. Marshall, "Elastic/Plastic Indentation Damage in Ceramics: The Median/Radial Crack System," *J. Am. Ceram. Soc.*, **63** [9–10] 574–81 (1980).
[28]E. R. Fuller, B. R. Lawn, and R. F. Cook, "Theory of Fatigue for Brittle Flaws Originating from Residual Stress Concentrations," *J. Am. Ceram. Soc.*, **66** [5] 314–21 (1983).
[29]D. B. Marshall and B. R. Lawn, "Residual Stresses in Dynamic Fatigue of Abraded Glass," *J. Am. Ceram. Soc.*, **64** [1] C-6–C-7 (1981).
[30]H. Chai and B. R. Lawn, "Role of Adhesive Interlayer in Transverse Fracture of Brittle Layer Structures," *J. Mater. Res.*, **15** [4] 1017–24 (2000).
[31]T. P. Dabbs, B. R. Lawn, and P. L. Kelly, "A Dynamic Fatigue Study of Soda–Lime and Borosilicate Glasses Using Small-Scale Indentation Flaws," *Phys. Chem. Glasses*, **23** [2] 58–66 (1982).
[32]B. R. Lawn, "Hertzian Fracture in Single Crystals with the Diamond Structure," *J. Appl. Phys.*, **39** [10] 4828–36 (1968).
[33]J. E. Ritter and M. R. Lin, "Effect of Polymer Coatings on the Strength and Fatigue Behavior of Indented Soda–Lime Glass," *Glass Tech.*, **32** [2] 51–54 (1991). □